

Intestinal Metabolite Compound K of Ginseng Saponin Potently Attenuates Metastatic Growth of Hepatocellular Carcinoma by Augmenting Apoptosis via a Bid-Mediated Mitochondrial Pathway

GANG SONG,^{*,†} SHIGUANG GUO,[†] WEIWEI WANG,[†] CHUN HU,[†] YUBING MAO,[‡]
 BING ZHANG,[‡] HONG ZHANG,^{†,§} AND TIANHUI HU^{*,†}

[†]Cancer Research Center, and [‡]Department of Basic Medical Sciences, Medical College of Xiamen University, Xiamen 361005, China, and [§]Tumor Biology, School of Life Sciences University of Skövde, SE-541 28 Skövde, Sweden

It was recently shown that compound K (CK), an intestinal bacterial metabolite of ginseng saponin, exhibits antihepatocellular carcinoma (HCC) activity, and Bid is a potential drug target for HCC therapy. This paper reports a novel mechanism of CK-induced apoptosis of HCC cells via Bid-mediated mitochondrial pathway. CK dramatically inhibited HCC cells growth in concentration- and time-dependent manners, and a high dose of CK could induce HCC cell apoptotic cell death. Furthermore, the effective dose of CK potently attenuated the subcutaneous tumor growth and spontaneous HCC metastasis *in vivo*. At the molecular level, immunohistochemical staining revealed that Bid expression in subcutaneous tumor and liver metastasis tissues decreased dramatically in CK-treated groups compared to untreated controls, which also implies that Bid may play a critical role in the growth and progression of HCC. Further study shows that translocation of full-length Bid to the mitochondria from nuclei during cytotoxic apoptosis was associated with the release of cytochrome *c* from mitochondria, indicating that full-length Bid is sufficient for the activation of mitochondrial cell death pathways in response to CK treatment in HCC cells. Taken together, the results not only reveal a Bid-mediated mitochondrial pathway in HCC cells induced by CK but also suggest that CK may become a potential cytotoxic drug targeting Bid in the prevention and treatment of HCC.

KEYWORDS: Ginseng saponin; compound K; hepatocellular carcinoma; Bid; apoptosis

INTRODUCTION

Bid, a BH3 domain-only pro-apoptotic molecule, is initially found to be cleaved by caspase-8 in response to death receptor-mediated apoptotic signaling (1, 2). The truncated Bid (tBid) is modified by myristoylation and translocated into mitochondria, where it activates oligomerization of Bak or Bax and induces cytochrome *c* release. Cytochrome *c* in turn activates the apoptotic cascade of caspases-9 and -3, leading to cell death (3, 4). The findings from our group and others have shown that the cleavage of Bid may not be an absolute requirement for Bid to be pro-apoptotic (5–8). Moreover, upon the administration of a high dose of DNA double-break agent causing irreparable damage to hepatocellular carcinoma (HCC), Bid is quickly translocated to the mitochondria to release cytochrome *c* (9). Thus, it can be seen that the Bid-mediated mitochondrial pathway is critical to apoptotic cell death initiated by external signals from other cells or by internal warnings resulting from cellular stresses. However, the functional mechanism of Bid-mediated mitochondrial pathway contributed to HCC chemotherapy is still largely unknown.

Compound K (CK), 20-*O*- β -D-glucopyranosyl-20(*S*)-protopanaxadiol (also known as IH901 and M1), is the main metabolite of protopanaxadiol type ginseng saponin by intestinal bacteria after oral administration of ginseng extract and is speculated to be the major form of protopanaxadiol saponins absorbed from the intestine (10–12). Previous studies showed that CK possesses various chemopreventive and chemotherapeutic activities, including attenuation of hepatic lipid accumulation (13), antigenotoxic and anticlastogenic activity (14), reverse multidrug resistance (15), and antimetastasis (16, 17). The effect of CK on the suppression of HCC cells survival has been studied in our previous work (18). However, the functional mechanisms of antiproliferation and apoptosis induced by CK in HCC cells are not clearly known.

Cancer is a growing health problem around the world, and HCC remains one of the most difficult tumors to treat, especially when the tumor is advanced or unresectable. Because there is only a narrow understanding of the molecular, cellular, and environmental mechanisms that drive disease pathogenesis, there are only limited therapeutic options (19). In the present study, using multiple *in vitro* and *in vivo* models, we examined the effect of CK on carcinogenesis and the development of HCC and explored the cellular and molecular mechanisms by which CK attenuated HCC development. Our study demonstrated that CK inhibited

*Authors to whom correspondence should be addressed [(G.S.) phone +86-592-2188275; fax +86-592-2186731; e-mail gangsongsd@xmu.edu.cn or (T.H.) thu@xmu.edu.cn].

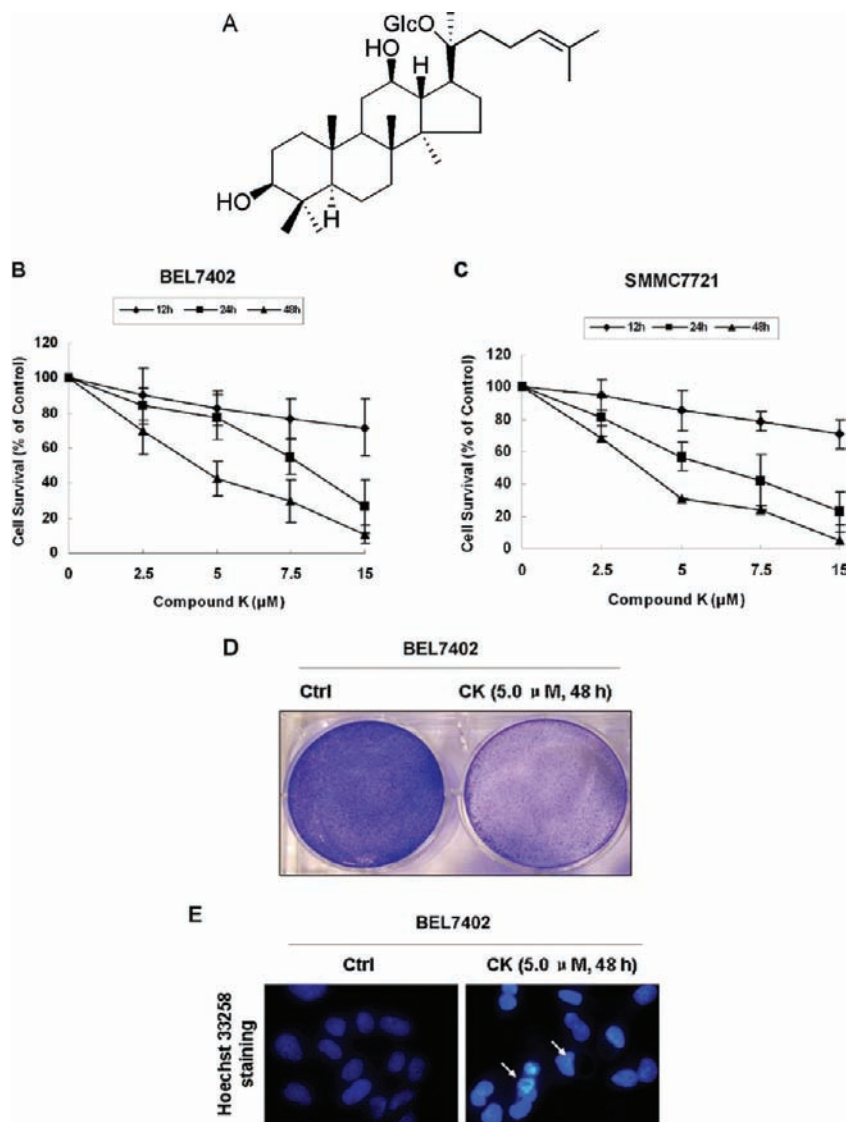


Figure 1. Effect of CK on the viability and morphology of HCC BEL7402 cells. **(A)** Chemical structure of CK. The structure is elucidated to be 20-*O*-(β -D-glucopyranosyl)-20(*S*)-protopanaxadiol. **(B, C)** Effect of CK on BEL7402 and SMMC7721 cell viabilities. The cell viabilities were determined by MTT assay. The data shown are means \pm SD of three separate experiments. **(D)** Surviving BEL7402 cells stained with Coomassie brilliant blue R 250 after 5.0 μM CK treatment for 48 h. **(E)** Morphology of BEL7402 cells and cells treated with 5.0 μM CK for 48 h. Cells were fixed and stained with Hoechst 33258, and the typical images were captured by fluorescence microscope (Leica DMIRB). The arrows indicate apoptotic cells or cells undergoing apoptosis.

cell survival and tumor growth through a Bid-mediated mitochondrial apoptotic pathway, which suggests CK may become a potentially therapeutic drug against HCC growth.

MATERIALS AND METHODS

Cell Culture and Cell Viability Assay. Human hepatocellular carcinoma BEL7402 and SMMC7721 cells were obtained from Shanghai Institute of Cell Biology, Chinese Academy of Sciences, Shanghai, China, and were maintained in DMEM supplemented with 10% FBS, 100 U/mL penicillin, and 100 $\mu\text{g}/\text{mL}$ streptomycin, at 37 $^{\circ}\text{C}$ in a humidified atmosphere of 95% air and 5% CO_2 . BEL7402 and SMMC7721 were regarded as poorly differentiated HCC lines established from surgical liver specimens in China. CK (>98% pure as determined by HPLC) was prepared and identified as in our previous publication (18) and dissolved in 0.1% dimethyl sulfoxide (DMSO). The structure of CK is shown in Figure 1A. Cell viability was assessed by MTT assay as previously described (20).

Cell Morphological Analysis. Cells were treated with 5.0 μM CK and 0.1% (v/v) DMSO (control) for 48 h, the cells were fixed with 4% paraformaldehyde and stained with Coomassie brilliant blue R 250, and then the morphological changes were observed under a phase-contrast microscope with a CCD camera (Leica DMIRB, Solms, Germany). In the other

experiment, some cells were incubated with 10 $\mu\text{g}/\text{mL}$ Hoechst 33258 (Sigma, St. Louis, MO). Thereafter, cell morphology was observed under a fluorescence microscope (Leica DMIRB).

Annexin V Assays. Cells were fed the CK media, and cells were serum-starved for 24 h as control group. At various time points, cells were harvested by trypsinization. After centrifugation, the cells were washed, resuspended, and stained for annexin V and PI as described in the manufacturer's instructions (Pharmingen, San Diego, CA). The samples were analyzed by Becton Dickinson FACScan (BD Biosciences, San Jose, CA).

Immunohistochemical Staining. The subcutaneous tumors and metastases were fixed in 10% formaldehyde and embedded in paraffin. Sections were then cut, and immunohistochemical staining was performed as previously described (21). As a negative control, the primary antibody was replaced with normal mouse IgG.

Immunofluorescence Double Staining. Immunofluorescence double staining was performed according to our previous description (8, 9) with some modifications. Briefly, after CK treatment, cells were fixed with 4% paraformaldehyde and permeabilized with 0.1% Triton X-100. Then, the fixed and permeabilized cells were incubated with the first primary antibody, mouse monoclonal antibody against Bid (1:200, Santa Cruz, CA). The cells were washed and subsequently incubated with a rabbit polyclonal antibody against Hsp60 (1:200, Santa Cruz, CA) for another 1 h

at room temperature. The cells were then washed and subsequently incubated with both FITC-conjugated goat anti-mouse and TRITC-conjugated goat anti-rabbit secondary antibodies (Santa Cruz, CA) at a dilution of 1:200 for 1 h at room temperature. After rinsing, the cells were mounted in ProLong Antifade solution onto glass slides. Stained cells were observed under fluorescence microscope (Leica DMIRB).

Cytosolic, Nuclear, and Mitochondrial Protein Isolation. The cytosolic, nuclear, and mitochondrial protein fractions were isolated according to our previously reported procedure (8, 9). Briefly, after treatment as indicated, cells were scraped in ice-cold homogenization buffer. The cells were then resuspended in 5 volumes of ice-cold extract buffer A (20 mM HEPES, 20 mM KCl, 1.5 mM MgCl₂, 1 mM EDTA, 1 mM EGTA, 1 mM DTT, 1 mM PMSF, 1 mM Na₃VO₃, pH 7.5, and 1× Protease Inhibitor Cocktail) and were homogenized. The homogenates were centrifuged at 750g for 10 min, and then the supernatant was collected and centrifuged at 10000g for 15 min to obtain the mitochondria pellets. The supernatants were further centrifuged at 100000g for 1 h to collect the supernatants (the cytosolic fraction). For the isolation of the nuclear protein, ice-cold extract buffer B (10 mM HEPES, 10 mM KCl, 1.5 mM MgCl₂, 0.5 mM DTT, 0.5 mM PMSF, 0.5 mM Na₃VO₃, pH 7.9, and 1× Protease Inhibitor Cocktail) was added to the pellet obtained after 750g centrifugation. The pellet and buffer B were mixed by gentle pipetting and kept in ice for 15 min. Ten percent Nondet NP-40 was then added and centrifuged at 10000g for 30 s. The supernatant was discarded, and the pellet was resuspended in extract buffer C. The pellet was homogenized and then centrifuged at 10000g for 20 min to collect the supernatant (the nuclear fraction).

Western Blot Analysis. Western blot was performed as in our previous publications (20). Protein Assay Kit for protein quantity analysis was purchased from Bio-Rad (Hercules, CA). The enhanced chemiluminescence (ECL) detection system was purchased from Amersham (Arlington Heights, IL). The mouse monoclonal antibody against cytochrome *c* was obtained from ZYMED1 Laboratories, Inc. (South San Francisco, CA). All other antibodies were provided by Santa Cruz (Santa Cruz, CA).

Xenograft Assays in Nude Mice. In vivo animal experiments with female Balb/c nude mice were conducted in accordance with the regulations of experimental animal administration and the animal ethical committee of the Medical College, Xiamen University. BEL7402 cells (2×10^6 /mice) were implanted by subcutaneous injection in the left flank of the mouse. To examine whether CK affects metastatic growth in the liver, BEL7402 cells (6×10^6 /mice) were injected into nude mice by intraportal vein injection as previously described (21). Then normal saline containing different concentrations of CK was administered to the mice by intraperitoneal injection every other day for 5 weeks. Mice in untreated control groups were given normal saline alone. Shortly after treatment of CK, all mice were killed and examined for the growth of subcutaneous tumors and micrometastasis formation. Six nude mice were used in each set of experiments.

Statistic Analysis. The data are presented as the mean \pm SD for at least three separate determinations for each group. Differences between the groups were examined for statistical significance using Student's *t* test with SPSS software.

RESULTS

CK Potently Attenuated Cell Viability in HCC Cells. To evaluate the cytotoxicity of CK (Figure 1A) on the proliferation of human HCC cells, we examined the effect of different concentrations of CK on cellular proliferation for 12, 24, and 48 h on BEL7402 and SMMC7721 cells by the MTT method. The growth inhibitory effects of CK against HCC cells are shown in Figure 1B,C. The results showed that CK significantly inhibits growth in concentration- and time-dependent manners. A significant loss of viability was detected in two HCC cell lines that were treated with $\geq 5.0 \mu\text{M}$ CK for 48 h. For example, the BEL7402 cell survival rates following dosage with $5.0 \mu\text{M}$ CK at 48 h amounted to $42.60 \pm 9.87\%$ compared to the control cells. We also examined the cell proliferation rate by BrdU-labeling assay, and similar results were observed (data was not shown). These results indicate that high concentrations of CK potently attenuate HCC cell viability (Figure 1B,C) but have little effect on the proliferation of cells that are treated with low concentrations of CK.

CK-Induced Apoptotic Cell Death in HCC Cells. To verify CK-induced apoptosis of HCC cells, we first examined the changes in cell morphology of BEL7402 after CK exposure under the phase contrast microscope. Forty-eight hours after exposure to $5.0 \mu\text{M}$ CK, HCC cells began to show cell shrinkage, rounding, and fragmentation and, thus, took on the typical appearance of apoptotic cells when compared to the untreated cells (Figure 1D). Then, we also analyzed cell morphological changes by Hoechst 33258 staining. The CK-treated cells also exhibited morphological changes indicative of apoptosis, including chromatin condensation and nuclear fragmentation (Figure 1E).

Two HCC cell lines, BEL7402 and SMMC7721, were used, and the flow cytometric measurement of cellular apoptosis by using annexin V levels revealed a consistent increase in apoptosis (Figures 2 and 3). After treatment with different concentrations of CK for 24 h, while the control group was serum-starved for 24 h, the results showed that CK induced apoptosis (annexin V levels of the cells) in a concentration-dependent manner (Figures 2A and 3A), respectively. Moreover, $5.0 \mu\text{M}$ CK induced HCC apoptosis in a time-dependent manner. For example, as shown in Figure 2B, the annexin V levels of BEL7402 cells after treatment with $5.0 \mu\text{M}$ CK for 36 h and the serum-starved control cells were 19.10 ± 2.91 and $7.91 \pm 1.02\%$, respectively (Figure 2B, $P < 0.05$). Similar results were observed in SMMC7721 cell experiments (Figure 3B). These results indicate that CK dramatically induced HCC cell apoptosis in concentration- and time-dependent manners. However, these observations were not fully consistent with the cell growth inhibition detected by MTT assay (Figure 1B,C). We believe that these differences are due to different detection systems.

To understand the mechanisms of how CK-induced HCC apoptotic cell death, we examined a number of relevant apoptotic proteins. As shown in Figures 2C and 3C, the Bak level in both control cells and CK treatment groups remained almost unchanged after 48 h of treatment, but the total cellular Bax level increased after 24 h with $5.0 \mu\text{M}$ CK treatment. In contrast with Bax, the total cellular Bcl₂ level had a slight decrease. More importantly, a significant decrease of Bid was detected after 24 h with $5.0 \mu\text{M}$ CK treatment in BEL7402 and SMMC7721 cells, suggesting Bid may be cleaved into a p15 form of tBid, which then translocated to mitochondria and mediated apoptosis. In addition, the typical procaspase-3 cleaved band was observed at 36 h after CK treatment in BEL7402 cells (Figure 2C), and the typical PARP cleaved band was observed at 24 h after CK treatment in SMMC7721 cells (Figure 3C).

CK Prominently Attenuated Xenograft Metastatic Growth in Nude Mice Transplanted with BEL7402 Cells. To further assess the biological significance of CK on the development of HCC, we investigated whether CK could alter the xenograft growth in nude mice transplanted with BEL7402 cells in vivo. As shown in Figure 4A,B, CK appeared to significantly attenuate the subcutaneous tumor growth over the controls, and the average tumor weight ratio of negative groups (saline normal) was > 3 -fold that in CK groups ($P < 0.05$). Meanwhile, subcutaneous tumor tissues were examined by H&E staining (Figure 4C, top panel), and Bid protein was analyzed by immunohistochemical staining. Tumors treated with 10.0 mg/kg CK showed obviously depressed expression of Bid (Figure 4C, bottom panel), together with the cellular debris and morphological changes associated with apoptosis. The result of Bid expression in immunohistochemical staining is in accordance with the significant decrease of Bid found by Western blot analysis in HCC cells treated with CK (Figures 2C and 3C).

Furthermore, we next examined whether the effective dose of CK could affect the metastatic potential and growth of the cancer cells in vivo. BEL7402 cells (6×10^6 /mice) were introduced into the nude mice via intraportal vein injection. Five weeks after the

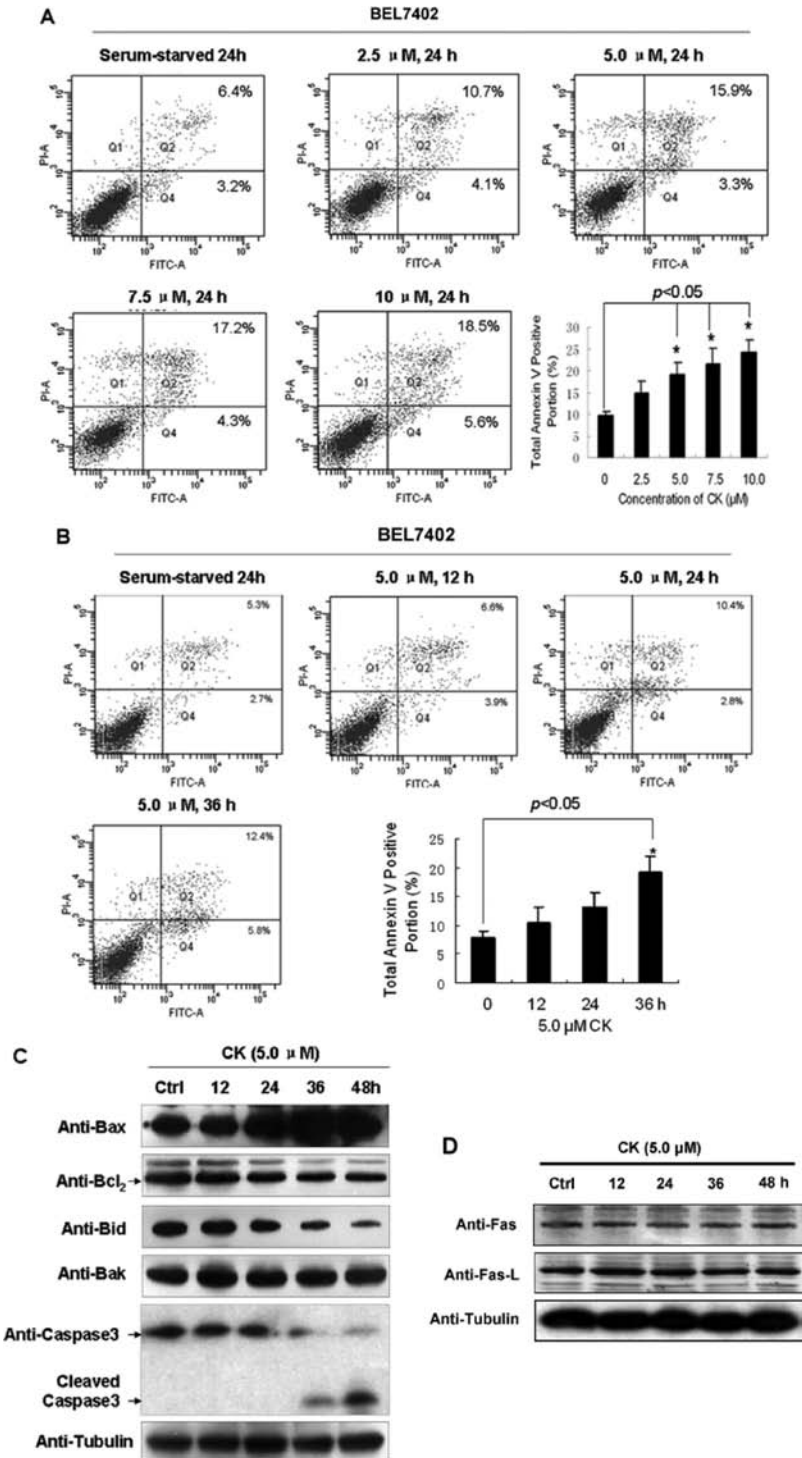


Figure 2. CK induced apoptotic cell death in HCC BEL7402 cells. BEL7402 cells were plated into triplicate wells of 6-well cell culture plates and treated with 2.5, 5.0, 7.5, or 10.0 μ M CK for 24 h (A) or treated with 5.0 μ M CK for 12, 24, or 36 h (B), respectively. The control group was serum-starved for 24 h. The cells were stained with annexin V and propidium iodide as the experimental procedures. Representative plots and average annexin V positive-PI negative percentages were determined by flow cytometric analysis. * indicates $P < 0.05$ compared with the control. (C, D) Effect of CK on the expression of apoptosis-related proteins, Fas and Fas-L, in BEL7402 cells. BEL7402 cells were treated with 5.0 μ M CK for 12, 24, 36, or 48 h, and then the total cell lysates were subjected to Western blotting analysis.

inoculation of tumor cells, the animals were sacrificed for the examination of metastatic growth. Strikingly, tumor metastases were detected in the liver of the negative groups (saline normal) (Figure 4D, left panel). In contrast, no visually observable metastatic tumors were found in the liver of CK groups (10.0 mg/kg) (Figure 4D, right panel). Tumor metastases in the liver of CK treatment group showed similarly depressed expression of Bid, which was also

analyzed by immunohistochemical staining (Figure 4E, bottom panel). Taken together, these results suggest that the effective dose of CK strongly attenuated tumor metastatic growth in vivo.

Distribution of Bid and Release of Cytochrome *c* in Response to CK Treatment. To further explore the functional mechanisms of Bid in human HCC cells in response to CK-induced apoptosis, we analyzed the cellular location and distribution of Bid following

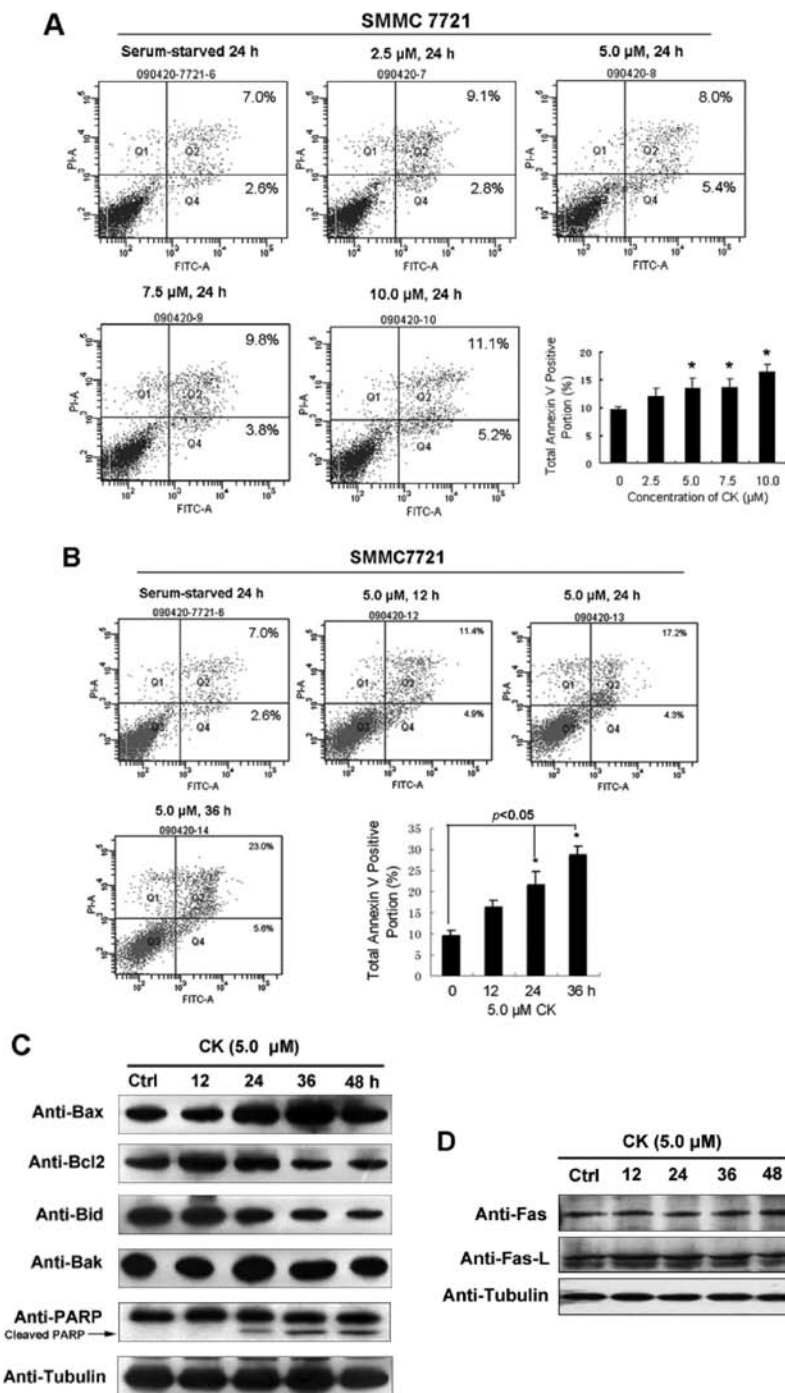


Figure 3. CK induced apoptotic cell death in HCC SMMC7721 cells. SMMC7721 cells were treated by CK at different concentrations for 24 h (A) or treated with 5.0 μ M CK for different periods times (B), respectively. The control group was serum-starved for 24 h. The cells were stained with annexin V and propidium iodide as the experimental procedures. Representative plots and average annexin V positive-PI negative percentages were determined by flow cytometric analysis. * indicates $P < 0.05$ compared with the control. (C, D) Effect of CK on the expression of apoptosis-related proteins, Fas and Fas-L, in SMMC7721 cells. SMMC7721 cells were treated with 5.0 μ M CK for 12, 24, 36, or 48 h, and then the total cell lysates were subjected to Western blotting analysis.

CK treatment. We first evaluated the subcellular localization of Bid following treatment of human HCC cells with 5.0 μ M CK by using immunofluorescence staining. As shown in Figure 5A, a portion of Bid protein was localized in the nuclei. However, following 5.0 μ M CK treatment for 48 h, consistent with typical mitochondrial protein Hsp60 (Figure 5A, middle panel), most of the Bid protein was distributed in the mitochondria and little was observed in the nuclei (Figure 5A, bottom left panel). Therefore, the distinct subcellular localization of Bid occurred in HCC cells treated with the effective doses of CK, indicating that the location

of Bid in HCC cells may be important for executing its apoptotic functions.

To further assess the subcellular localization of Bid in human HCC cells, we performed Western blotting analysis of subcellular fractionations. As shown in Figure 5B, after exposure of the human HCC cells on 5.0 μ M CK for 48 h, the endogenous Bid translocated from the nuclei to the mitochondria and the cytosol. This is in accordance with the localization of Bid observed by immunofluorescence staining (Figure 5A). In addition, accompanying the translocation of Bid to the mitochondria, the release

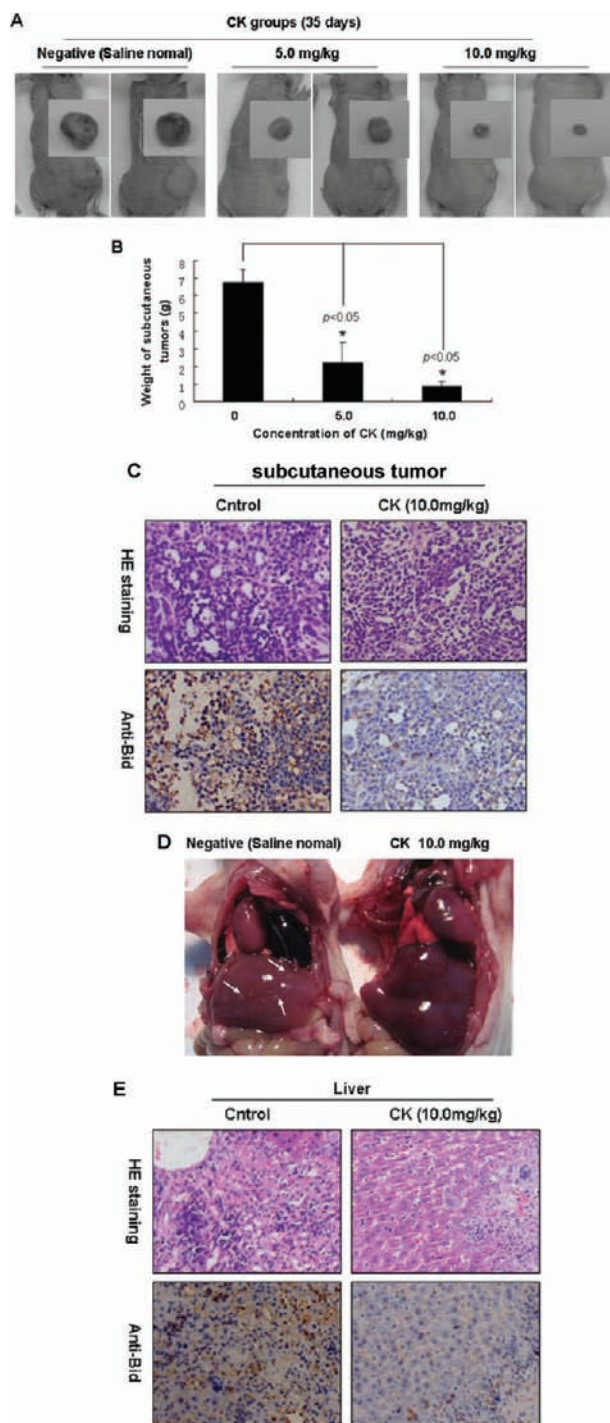


Figure 4. CK potently attenuated xenograft metastatic growth in nude mice transplanted with BEL7402 cells. **(A, B)** BEL7402 cells were injected into Balb/c nude mice via subcutaneous injection. Different doses of CK were administered to the mice by intraperitoneal injection every other day. Control groups were given normal saline alone. After 35 days, the mice were sacrificed and analyzed for tumor formation. * indicates $P < 0.05$ compared with the control groups. **(C)** The subcutaneous tumors of untreated and CK-treated nude mice were immunostained with anti-Bid antibody and analyzed by H&E staining. The positive staining for Bid protein is shown in brown color. All sections were counterstained with hematoxylin, shown in blue color. **(D)** Typical photographs of CK prominently attenuated tumor metastasis in the liver via intraportal vein injection as xenografts in nude mice. **(E)** Expression of Bid in the tumor metastasis of the liver tissues in nude mice by immunohistochemical and H&E staining analysis.

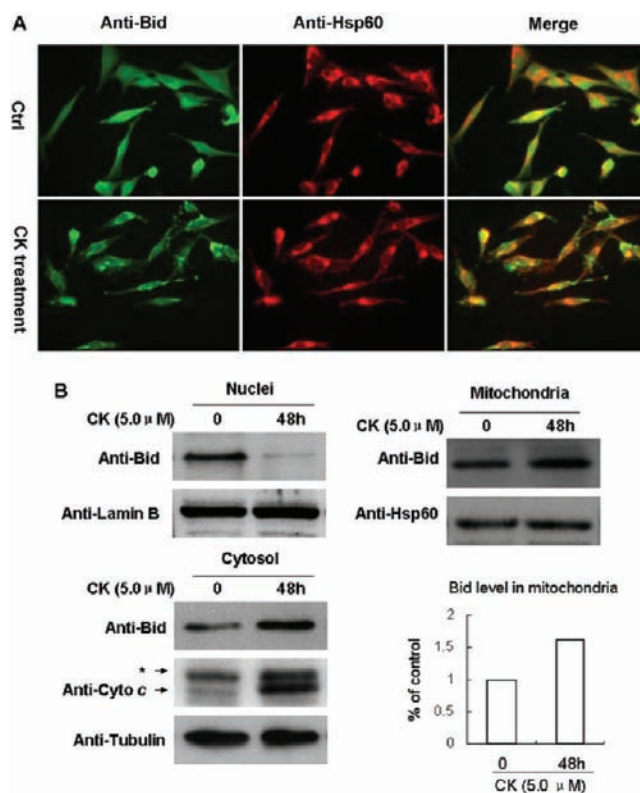


Figure 5. Translocation of Bid and cytochrome *c* release into the cytosol in response to CK treatment. **(A)** BEL7402 cells were immunostained with anti-Hsp60 and anti-Bid antibodies followed by the corresponding FITC- and TRITC-conjugated secondary antibodies to show the presence of Hsp60 and Bid proteins simultaneously. The fluorescent images were visualized with a fluorescence microscope. **(B)** Distribution of Bid and cytochrome *c* in the cytosolic, mitochondrial, and nuclear fractions by Western blot analysis. Tubulin, lamin B, and Hsp60 were used as the loading controls. * indicates nonspecific bands.

of cytochrome *c* from mitochondria to the cytosol was observed (**Figure 5B**). On the basis of the above results, Bid-mediated mitochondrial activation accompanying cytochrome *c* release may be a pivotal mechanism for CK-induced HCC apoptotic cell death (**Figure 6**).

DISCUSSION

Ginseng saponins have been widely reported to exert anticancer activity. CK is an intestinal bacterial metabolite of panaxoside. It has been reported to effectively inhibit the growth of a variety of tumor cells (23, 24). We have demonstrated that CK exerts an antiproliferation effect in HCC (18). However, the relationships between CK and HCC are not clearly understood. Especially, its molecular mechanisms on inducing apoptosis in HCC cells have not been reported. Therefore, here, we focused on the cellular location and distribution of Bid, a key molecule in the process of CK-induced apoptosis in BEL7402, a HCC cell line with high metastatic potentials.

Cancer cells, including HCC, commonly resist cell death through either disruption of apoptotic processes or activation of survival signals. Our previous study showed that CK inhibited the cell growth of HepG2 and MHCC97-H HCC cell lines in a concentration- and time-dependent manner (18). In this study, we first found that CK could significantly inhibit the viabilities of HCC cell lines BEL7402 and SMMC7721 in a concentration–time-dependent manner. To clarify whether CK can induce apoptosis in HCC cells, Hoechst33342 staining and annexin-V/PI staining assays showed that CK could apparently induce HCC cell apoptosis.

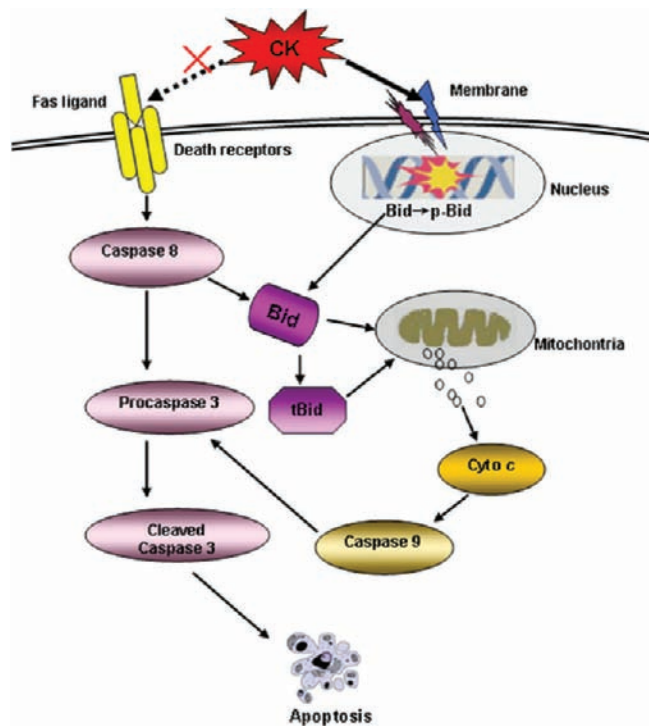


Figure 6. Hypothetical illustration of metastatic growth attenuation of hepatocellular carcinoma by CK via Bid-mediated mitochondrial pathway.

There are two classic apoptotic pathways in mammalian cells, namely, an internal pathway and an external pathway, also known as the mitochondria-mediated apoptotic pathway and the death receptor-mediated apoptotic pathway. Accumulated reports suggest that they have cross-talk. Some studies found that the mechanisms on CK-induced tumor cell apoptosis are both involved in the two apoptotic pathways (24, 25). To further clarify the apoptotic molecular mechanisms of HCC cells induced by CK treatment, we analyzed a series of apoptosis-related protein expression in the total proteins of HCC BEL7402 and SMMC7721 cells treated with CK for different periods using a Western blotting assay. The most important result we found is that the expression level of Bid was down-regulated significantly, and pro-caspase-3 and PARP showed cleavage activation after CK treatment. Furthermore, cytochrome *c* expressions in cytoplasm induced by CK were also detected (Figure 5B). However, we did not observe the significant change of expression levels of Fas and Fas-L (Figures 2D and 3D). In addition, we could not observe the cleaved Bid (tBid, 15 KD) expression in the total or mitochondrial protein by Western blotting analysis. We believe that tBid protein is unstable, and it promotes ubiquitin degradation easily. Taken together, these results show that CK induces apoptosis in HCC cells mainly through the Bid-mediated mitochondria internal pathway. It is worth mentioning that the total expression rate of Bax/Bcl-2 might partly indicate the fate of cells. Our study demonstrated that CK up-regulated pro-apoptotic Bax protein expression in a time-dependent manner. These results suggest that pro-apoptotic Bax proteins might also play an important role in CK-induced HCC cell apoptosis.

Bid is a BH3-only Bcl2 family member with multiple functions. First, Bid has emerged as a central player linking death signals through surface death receptors to the core apoptotic mitochondrial pathway (26). According to previous studies, full-length Bid is sufficient for the activation of mitochondrial cell death pathways in response to internal and external signals. Here, we provide solid evidence suggesting pro-apoptotic effects of CK in HCC mediated

by full-length Bid. Recently, using other cell lines, Cho et al. reported similar results and hypothesized that pro-apoptotic effects of CK (10–20 μ M) could be linked to the activation of caspases-3, -8, and -9, the loss of mitochondrial membrane potential, the release of cytochrome *c* and Smac/DIABLO to the cytosol, the translocation of Bid and Bax to mitochondria, and the down-regulations of Bcl-2 and Bcl-xL (27). On the other hand, Choi et al. reported that CK induced tumor-specific apoptotic cell death of human malignant astrocytoma cells via the intrinsic pathway along with the involvement of the mitochondria (28). Furthermore, most recently Kim et al. also demonstrated that CK exhibited cytotoxic effects via AMPK activation, ROS generation, and induction of apoptosis (29). To show the clear site-specific effect of Bid in human carcinoma cells by CK treatment, we combined immunofluorescence and cell fractionation methods. In morphology, Hsp60 was chosen as a specific mitochondrial marker. Our data showed that Bid was localized in both the cytosol and the nucleus of HCC cells that were not subjected to CK treatment. After treatment with 5.0 μ M CK, most of the Bid protein was distributed in the mitochondria, and little was observed in the nucleus. This difference in the subcellular localization of Bid in HCC cells indicates that the location of Bid in cells may be important to the execution of its pro-apoptotic function. To further assess the subcellular localization of Bid in HCC cells, we performed Western blotting analysis of the subcellular fractionations of Bid (Figure 5B). The results showed that endogenous Bid translocated from the nuclei to the mitochondria and the cytosol, and this is in agreement with the localization of Bid observed by immunofluorescence staining. In particular, our concern is the nuclear Bid translocation occurring by CK treatment, and this biological process performed possibly by the assistance of p53 (8). In addition to the translocation of Bid to the mitochondria, the release of cytochrome *c* from the mitochondria to the cytosol was observed, which is a clear marker of mitochondrial alterations in apoptosis. Our data therefore clarify the molecular mechanisms of Bid-mediated apoptosis of HCC cells in response to CK treatment.

In conclusion, the present studies demonstrated that CK, a novel ginseng saponin metabolite, could significantly inhibit proliferation and induce apoptosis in human HCC cells via a Bid-mediated mitochondrial pathway, which may be a pivotal mechanism for CK-induced HCC apoptotic cell death. The elucidation of the mechanism of Bid points to CK-induced apoptosis, suggesting a possible therapeutic option of CK or potential of combination with other chemotherapies targeting Bid to treat HCC.

ABBREVIATIONS USED

BH, Bcl2-homology region; Bid, BH3-interacting domain death agonist; BSA, bovine serum albumin; CK, compound K; DMSO, dimethyl sulfoxide; FBS, fetal bovine serum; HCC, hepatocellular carcinoma; H&E, hematoxylin and eosin; MTT, 3-(4,5-dimethylthiazol-2-yl)-2,5-diphenyltetrazolium bromide; PBS, phosphate-buffered saline; PI, propidium iodide; tBid, truncated Bid.

LITERATURE CITED

- Wang, K.; Yin, X. M.; Chao, D. T.; Milliman, C. L.; Korsmeyer, S. J. BID: a novel BH3 domain-only death agonist. *Genes Dev.* **1996**, *10*, 2859–2869.
- Yin, X. M. Bid, a BH3-only multi-functional molecule, is at the cross road of life and death. *Gene* **2006**, *369*, 7–19.
- Li, H.; Zhu, H.; Xu, C. J.; Yuan, J. Cleavage of BID by caspase 8 mediates the mitochondrial damage in the Fas pathway of apoptosis. *Cell* **1998**, *94*, 491–501.
- Luo, X.; Budihardjo, I.; Zou, H.; Slaughter, C.; Wang, X. Bid, a Bcl-2 interacting protein, mediates cytochrome *c* release from mitochondria in response to activation of cell surface death receptors. *Cell* **1998**, *94*, 481–490.

- (5) König, H. G.; Rehm, M.; Gudorf, D.; Krajewski, S.; Gross, A.; Ward, M. W.; Prehn, J. H. Full length Bid is sufficient to induce apoptosis of cultured rat hippocampal neurons. *BMC Cell Biol.* **2007**, *8*, 7–14.
- (6) Sarig, R.; Zaltsman, Y.; Marcellus, R. C.; Flavell, R.; Mak, T. W.; Gross, A. BID-D59A is a potent inducer of apoptosis in primary embryonic fibroblasts. *J. Biol. Chem.* **2003**, *278*, 10707–10715.
- (7) Valentijn, A. J.; Gilmore, A. P. Translocation of full-length Bid to mitochondria during anoikis. *J. Biol. Chem.* **2004**, *279*, 32848–32857.
- (8) Song, G.; Chen, G. G.; Yun, J. P.; Lai, P. B. S. Association of p53 with Bid induces cell death in response to etoposidetreatment in hepatocellular carcinoma. *Curr. Cancer Drug Targets* **2009**, *9*, 871–880.
- (9) Song, G.; Chen, G. G.; Chau, D. K.; Miao, J.; Lai, P. B. Bid exhibits S phase checkpoint activation and plays a pro-apoptotic role in response to etoposide-induced DNA damage in hepatocellular carcinoma cells. *Apoptosis* **2008**, *13*, 693–701.
- (10) Karikura, M.; Miyase, T.; Tanizawa, H.; Taniyama, T.; Takino, Y. Studies on absorption, distribution, excretion and metabolism of ginseng saponins. VII. Comparison of the decomposition modes of ginsenoside-Rb1 and -Rb2 in the digestive tract of rats. *Chem. Pharm. Bull. (Tokyo)* **1991**, *39*, 2357–2361.
- (11) Hasegawa, H.; Sung, J. H.; Matsumiya, S.; Uchiyama, M. Main ginseng saponin metabolites formed by intestinal bacteria. *Planta Med.* **1996**, *62*, 453–457.
- (12) Akao, T.; Kanaoka, M.; Kobashi, K. Appearance of compound K, a major metabolite of ginsenoside Rb1 by intestinal bacteria, in rat plasma after oral administration – measurement of compound K by enzyme immunoassay. *Biol. Pharm. Bull.* **1998**, *21*, 245–249.
- (13) Kim, D. Y.; Yuan, H. D.; Chung, I. K.; Chung, S. H. Compound K, intestinal metabolite of ginsenoside, attenuates hepatic lipid accumulation via AMPK activation in human hepatoma cells. *J. Agric. Food Chem.* **2009**, *57*, 1532–1537.
- (14) Lee, B. H.; Lee, S. J.; Hur, J. H.; Lee, S.; Sung, J. H.; Huh, J. D.; Moon, C. K. *In vitro* antigenotoxic activity of novel ginseng saponin metabolites formed by intestinal bacteria. *Planta Med.* **1998**, *64*, 500–503.
- (15) Hasegawa, H.; Sung, J. H.; Matsumiya, S.; Uchiyama, M.; Inouye, Y.; Kasai, R.; Yamasaki, K. Reversal of daunomycin and vinblastine resistance in multidrug-resistant P388 leukemia in vitro through enhanced cytotoxicity by triterpenoids. *Planta Med.* **1995**, *61*, 409–413.
- (16) Hasegawa, H.; Jong, H. S.; Jae, D. H. Ginseng intestinal bacterial metabolite IH901 as a new antimetastatic agent. *Arch. Pharm. Res.* **1997**, *6*, 539–544.
- (17) Choo, M. K.; Sakurai, H.; Kim, D. H.; Saiki, I. A ginseng saponin metabolite suppresses tumor necrosis factor- α -promoted metastasis by suppressing nuclear factor- κ B signaling in murine colon cancer cells. *Oncol. Rep.* **2008**, *19*, 595–600.
- (18) Ming, Y. L.; Song, G.; Chen, L. H.; Zheng, Z. Z.; Chen, Z. Y.; Ouyang, G. L.; Tong, Q. X. Anti-proliferation and apoptosis induced by a novel intestinal metabolite of ginseng saponin in human hepatocellular carcinoma cells. *Cell Biol. Int.* **2007**, *31*, 1265–1273.
- (19) Di Maio, M.; De Maio, E.; Perrone, F.; Pignata, S.; Daniele, B. Hepatocellular carcinoma: systemic treatments. *J. Clin. Gastroenterol.* **2002**, *35*, S109–S114.
- (20) Song, G.; Mao, Y. B.; Cai, Q. F.; Yao, L. M.; Ouyang, G. L.; Bao, S. D. Curcumin induces human HT-29 colon adenocarcinoma cell apoptosis via activating p53 and regulating apoptosis-related proteins. *Braz. J. Med. Biol. Res.* **2005**, *38*, 1791–1798.
- (21) Song, G.; Ouyang, G.; Mao, Y. B.; Ming, Y. L.; Bao, S.; Hu, T. H. Osteopontin promotes metastatic growth of gastric cancer by augmenting cell survival and invasion through Akt-mediated HIF-1 α up-regulation and MMP9 activation. *J. Cell Mol. Med.* **2009**, *13*, 1706–1718.
- (22) Chae, S.; Kang, K. A.; Chang, W. Y.; Kim, M. J.; Lee, S. J.; Lee, Y. S.; Kim, H. S.; Kim, D. H.; Hyun, J. W. Effect of compound K, a metabolite of ginseng saponin, combined with γ -ray radiation in human lung cancer cells in vitro and in vivo. *J. Agric. Food Chem.* **2009**, *57*, 5777–5782.
- (23) Kim, D. Y.; Park, M. W.; Yuan, H. D.; Lee, H. J.; Kim, S. H.; Chung, S. H. Compound K induces apoptosis via CAMK-IV/AMPK pathways in HT-29 colon cancer cells. *J. Agric. Food Chem.* **2009**, *57*, 10573–10578.
- (24) Oh, S. H.; Lee, B. H. A ginseng saponin metabolite-induced apoptosis in HepG2 cells involves a mitochondria-mediated pathway and its downstream caspase-8 activation and Bid cleavage. *Toxicol. Appl. Pharmacol.* **2004**, *194*, 221–229.
- (25) Park, E. J.; Zhao, Y. Z.; Kim, J.; Sohn, D. H. A ginsenoside metabolite, 20-O- β -D-glucopyranosyl-20(S)-protopanaxadiol, triggers apoptosis in activated rat hepatic stellate cells via caspase-3 activation. *Planta Med.* **2006**, *72*, 1250–1253.
- (26) Song, G.; Chen, G. G.; Hu, T. H.; Lai, P. B. Bid stands at the crossroad of stress-response pathways. *Curr. Cancer Drug Targets* **2010**, *10*, 584–592.
- (27) Cho, S. H.; Chung, K. S.; Choi, J. H.; Kim, D. H.; Lee, K. T. Compound K, a metabolite of ginseng saponin, induces apoptosis via caspase-8-dependent pathway in HL-60 human leukemia cells. *BMC Cancer* **2009**, *9*, 49.
- (28) Choi, K.; Choi, C. Proapoptotic ginsenosides compound K and Rh enhance Fas-induced cell death of human astrocytoma cells through distinct apoptotic signaling pathways. *Cancer Res. Treat.* **2009**, *41*, 36–44.
- (29) Kim, A. D.; Kang, K. A.; Zhang, R.; Lim, C. M.; Kim, H. S.; Kim, D. H.; Jeon, Y. J.; Lee, C. H.; Park, J.; Chung, W. Y.; Hyun, J. W. Ginseng saponin metabolite induces apoptosis in MCF-7 breast cancer cells through the modulation of AMP-activated protein kinase. *Environ. Toxicol. Pharmacol.* **2010**, *30*, 134–140.

Received for review October 1, 2010. Revised manuscript received November 12, 2010. Accepted November 14, 2010. This work was supported by grants from the National Natural Science Foundation of China (No. 31071187 and 30971524), the Natural Science Foundation of Fujian province (2010J06015), the Fundamental Research Funds for the Central Universities (2010121102), and the special fund for public welfare research institutes of Fujian Province (2010R1101).